

Understanding the Lithium Storage Mechanism in Core-Shell Fe₂O₃@C Hollow Nanospheres Derived from Metal-Organic Frameworks: An *In operando* Synchrotron Radiation Diffraction and *in operando* X-ray Absorption Spectroscopy Study

Chengping Li,[†] Angelina Sarapulova,[†] Zijian Zhao,[†] Qiang Fu,[†] Vanessa Trouillet,^{†,‡} Aleksandr Missiul,[#] Edmund Welter,[†] and Sonia Dsoke *^{†,§}

[†] Institute for Applied Materials (IAM), Karlsruhe Institute of Technology (KIT), Hermann-von-Helmholtz-Platz 1, 76344 Eggenstein-Leopoldshafen, Germany.

[‡] Karlsruhe Nano Micro Facility (KNMF), Karlsruhe Institute of Technology (KIT), Hermann-von-Helmholtz-Platz 1, Eggenstein-Leopoldshafen, 76344, Germany

[§]Helmholtz Institute Ulm for Electrochemical Energy Storage (HIU), Helmholtzstraße 11, 89081 Ulm, Germany

[#] CELLS-ALBA Synchrotron, Cerdanyola del Valles, E-08290 Barcelona, Spain

[†]Deutsches Elektronen-Synchrotron DESY -A Research Centre of the Helmholtz Association, Notkestraße 85, D-22607 Hamburg, Germany

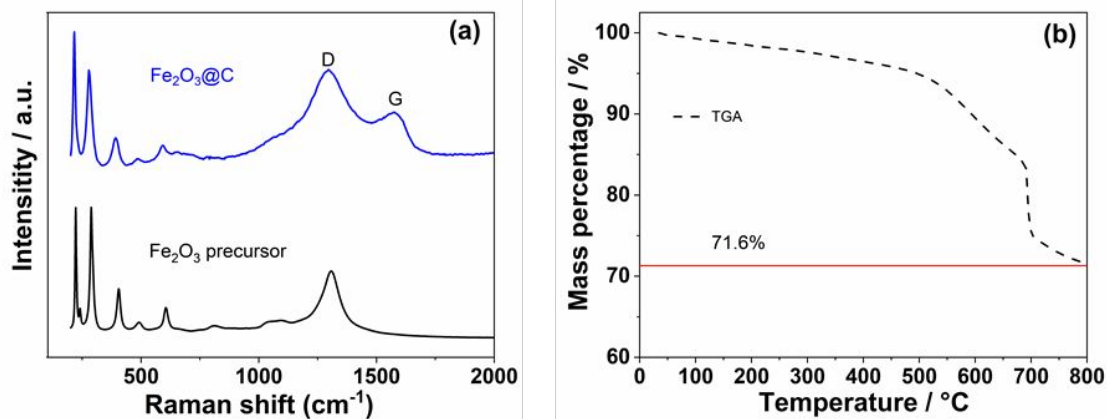


Figure S1. (a) The Raman spectra of the Fe₂O₃ precursor and Fe₂O₃@C and (b) TGA curve of the Fe₂O₃@C composite material.

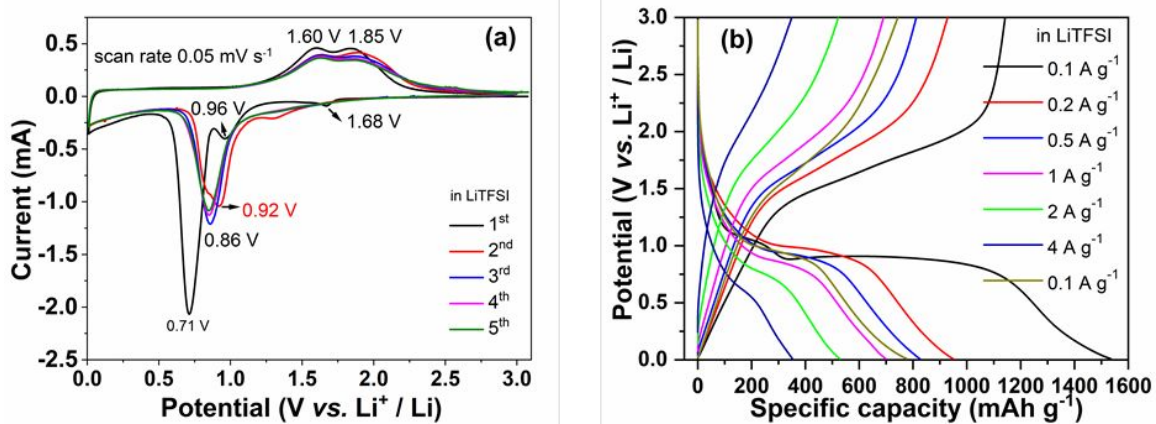


Figure S2. (a) CV profiles of the 1st to 5th for the Fe₂O₃@C at a sweep rate of 0.05 mV s⁻¹ in LiTFSI. (b) The galvanostatic profiles at various current densities in LiTFSI.

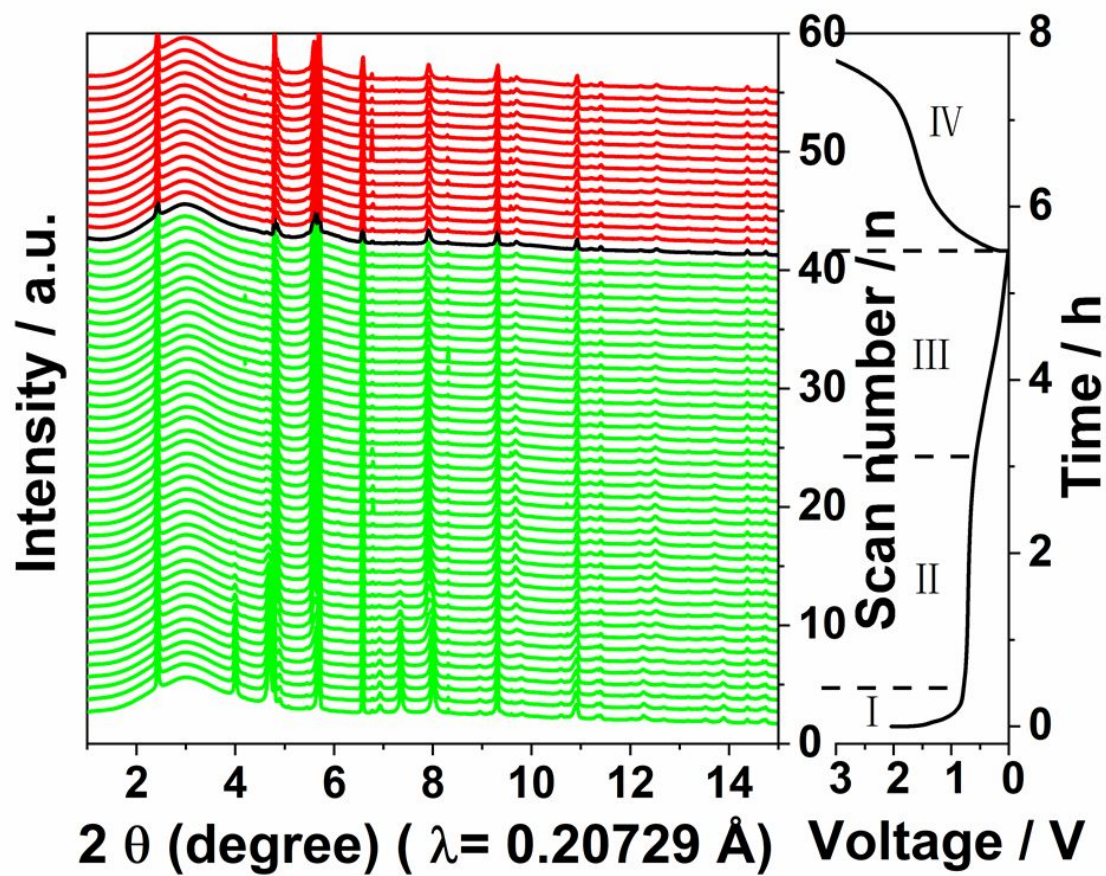


Figure S3. *In operando* XRD investigate of the lithium storage mechanism of the $\text{Fe}_2\text{O}_3@\text{C}$ electrode: The structural evolution during the first lithiation /de-lithiation processes in LiTFSI.

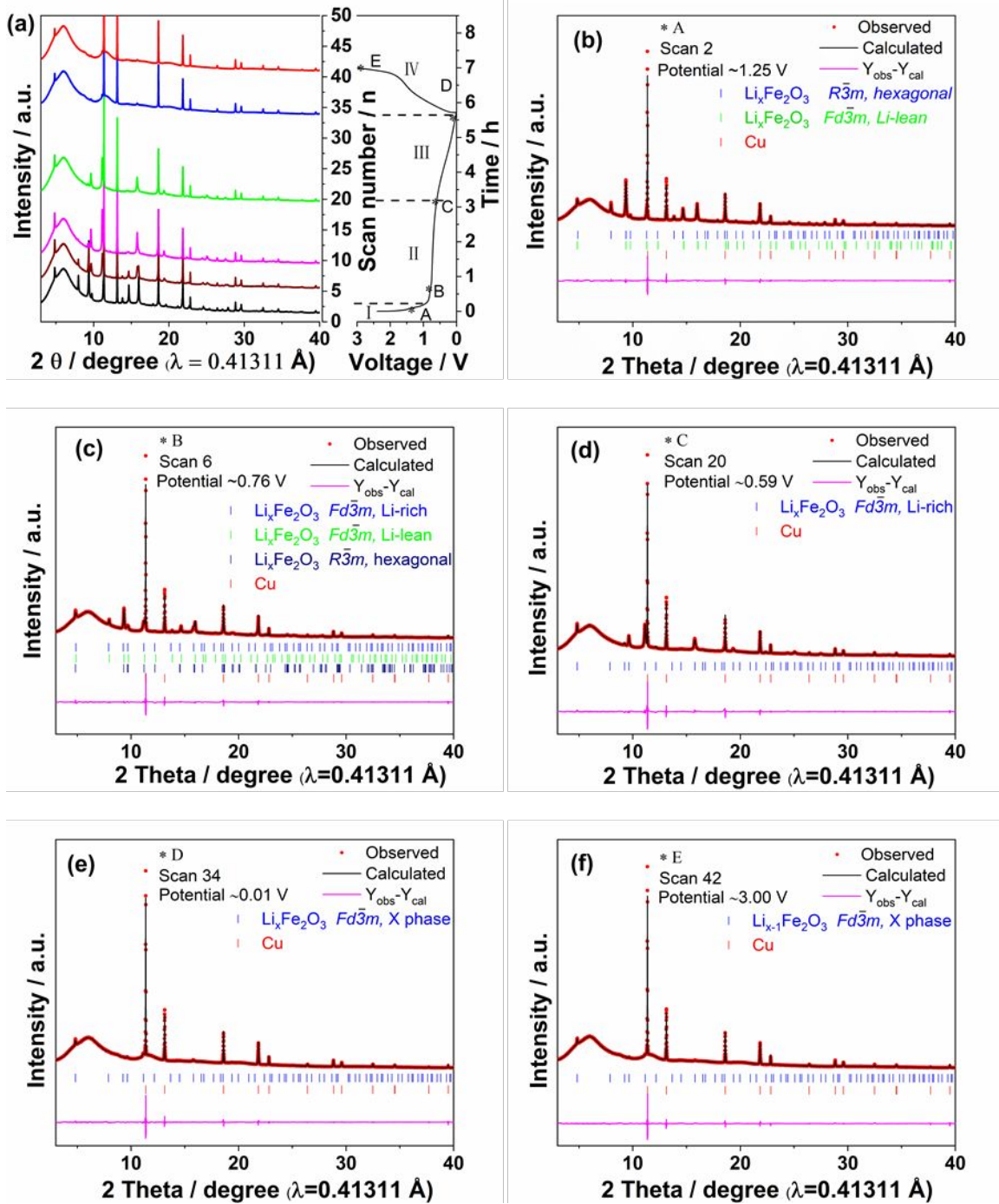


Figure S4. (a) *In operando* SRD patterns of the Fe₂O₃@C electrode was collected at various potential states. The Rietveld refinement results of the electrode at some selected potentials (A-E): the 1st lithiation to 1.25 V (b), 0.76 V (c), 0.59 V (d), 0.01 V (e), and the 1st de-lithiation to 3.00 V (f).

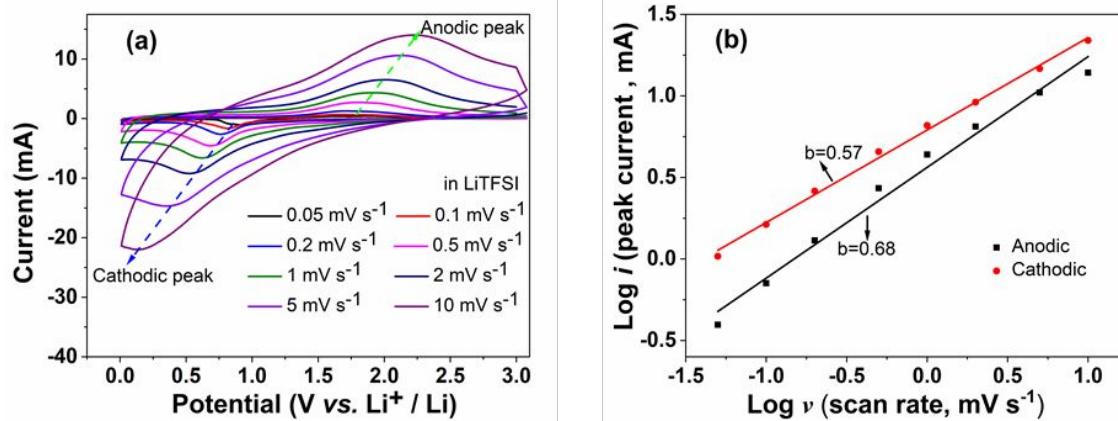


Figure S5. Kinetics characterization of the $\text{Fe}_2\text{O}_3@\text{C}$ electrode in LiTFSI: (a) CV profiles with scan rates between 0.05 to 10 mV s^{-1} . (b) The linear relationship of $\text{log } i$ (peak current) vs. $\text{log } \nu$ (scan rate) for anodic and cathodic peaks.

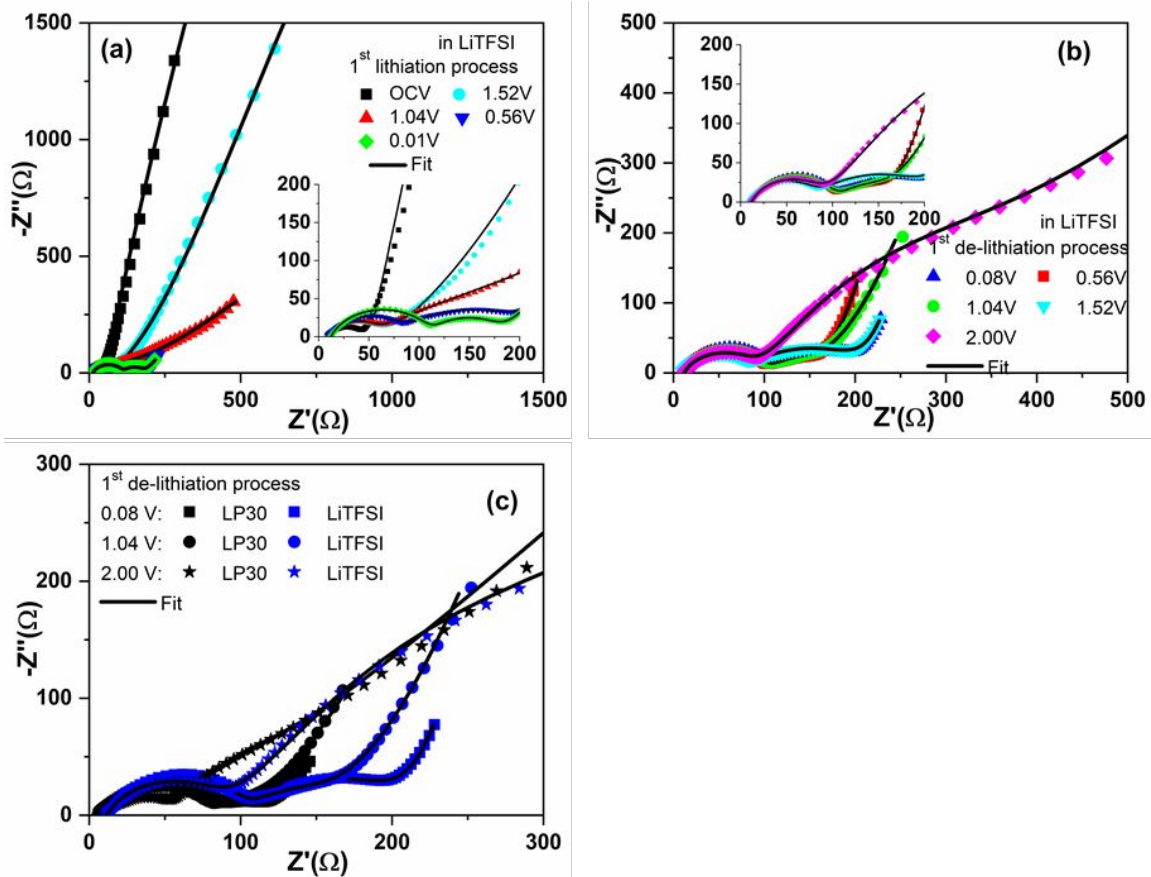


Figure S6. Nyquist plots of the $\text{Fe}_2\text{O}_3@\text{C}$ electrode measured on the freshly assembled cell (OCV) and at selected potentials during the first lithiation (a) and de-lithiation (b) processes in LiTFSI. Comparison of the Nyquist plots of $\text{Fe}_2\text{O}_3@\text{C}$ electrode was evaluated at 2.0, 1.04, and 0.01 V vs. Li^+/Li during the de-lithiation process in LP30 and LiTFSI (c).